Proceedings of the
International Conference on Mechanical Engineering 2011
(ICME2011) 18-20 December 2011, Dhaka, Bangladesh

ICME11–FL-053

STUDY OF AC ELECTROOSMOTIC FLOW DEVELOPED BY CO-PLANAR MICROELECTRODE ARRAY IN A SLIT MICROCHANNEL

Naheed Ferdous, Tariq Mahbub and Noor Quddus

Department of Mechanical Engineering, Bangladesh University of Engineering and Technology, Dhaka-1000, Bangladesh

ABSTRACT

Under the influence of an AC electric field, electrolytes on a planar microelectrodes exhibit steady fluid flow, termed as AC electro-osmosis. A numerical model using finite element scheme has been developed to solve the electrokinetic flow parameters of the AC electroosmosis in a slit microchannel. The solution was obtained using Poisson–Navier–Stokes–Nernst–Planck approach known as non equilibrium model. A thin-layer, low-frequency, nonlinear analysis of the system is performed including Faradaic currents from electrochemical reactions at the electrodes. Net flow velocity is observed for different geometric parameters of electrodes. Flow and field characteristic are observed for the maximum velocity attained in the investigated range of frequency. The interesting consequences of shape and field asymmetries, which generally lead to electro-osmotic pumping or electrophoretic motion in AC fields gives some basic issues for the microfluidic devices..

Keywords: AC Electroosmosis, Microelectrode, Poisson-Nernst-Planck, Faradaic Current.

1. INTRODUCTION

Alternating electric fields can generate a net steady motion of aqueous saline solutions over microelectrode structures. The term *ac electro-osmosis* (ACEO) refers to the fluid motion generated on top of electrodes by the interaction between an ac electric field and electrical charge that this field induces at the electrode/electrolyte interface i.e. charge induced in electrical double layer. The mechanism of ac electro-osmotic driven fluid flow has recently been shown to be capable of producing unidirectional pumping of liquid on a microscale, on asymmetric pairs of coplanar microelectrodes as demonstrated experimentally [1], theoretically [2], and numerically [3]. Electrical forces are used to transport, mix, separate, and manipulate various molecular or colloidal entities in microfluidic chips [4-5]. Experimental results are compared with a simple model based on the interaction of the non-uniform electric field [6-8]. At low potentials, the predicted velocities are in reasonable agreement with the experiments. Two different models for the simulation of the ac electroosmotic flow in a microchannel have been discussed where simplified model leads to a fast stationary solution and the second model has analyzed all essential processes in the time domain [9]. However, Faradaic currents can occur in such systems as a result of electrochemical reactions. A nonequilibrium 1D mathematical model of an ac electroosmotic system with electrochemical reactions is presented in [10]. Linear and weakly nonlinear theoretical studies were done for fluid flow [11]. The effect of Faradaic currents on the electroosmotic slip velocity generated at the electrode/electrolyte interface is taken over the assumption of perfectly polarizable electrodes. Theoretical results are applied for analyzing the influence of Faradaic reactions on AC electroosmotic flows [12]. The combined action of two experimentally relevant effects, i.e. Faradaic currents from electrochemical reactions at the electrodes and differences in ion mobilities of the electrolyte is taken into account in the analyses of ac electro-osmosis [13]. Approximation made are negligible advective currents, linearization of PNP equations, thin layer approximation etc. Because of these approximations, the results obtained are partial explanation of the mechanisms underlying ac electro-osmosis with Faradaic currents. A complete analysis must be fully nonlinear. Motivated by this, in order to extend previous theoretical analysis of Faradaic currents in ACEO by considering a symmetric electrolyte with ions of different mobilites, a low-frequency, complete nonlinear analysis of the

system including Faradaic currents from electrochemical reactions at the electrodes is performed in the present study.

2. FORMULATION OF THE PROBLEM

2.1 Geometry

A coplanar arrangement of ac electroosmotic pump as shown in Fig 1 is considered. The studied microfluidic pump can be represented by a single segment of a long microfluidic channel. We assume that a microchannel consists of an infinitely large series of segments with periodic boundary conditions. The micro channel width is much larger than the other characteristic dimensions of the segments, so the ac electroosmotic pump can be described as a 2-D object with length L and height H. The electrodes have lengths E_1 and E_2, and they are separated by two gaps, namely, G_1 and G_2. A 1:1 aqueous solution X^+Y^- e.g., H^+Cl^- placed on top of an array of electrodes subjected to an ac signal. Above this plane, three distinct layers are distinguished: compact, diffuse, and diffusion.

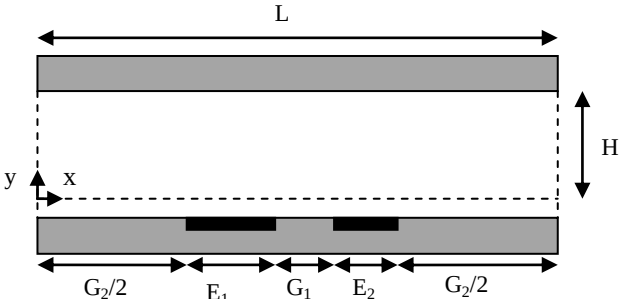

Fig 1. Schematic Diagram of the Physical Domain

2.2 Governing Equation

Two charged species are included in this model and the pair of ions are considered to be *asymmetric* in the sense that their mobilities are different. For simplicity, it is assumed that the cations react reversibly at the electrodes to produce neutral molecules according to a simple one-step one-electron redox process of the form $X^+ + e^- \leftrightarrow X$ and that the electrodes are blocking for the anions. The electric potential obeys Poisson's equation,

$$\varepsilon \nabla^2 \phi = -q,\ q = F(c^+ - c^-) \tag{1}$$

The particle densities satisfy Nernst-Planck equations,

$$\frac{\partial c^+}{\partial t} = -\nabla \cdot \mathbf{J}^+,\ \mathbf{J}^+ = \mathbf{u}c^+ - D^+(\nabla c^+ - c^+ \frac{F}{RT}\nabla\phi) \tag{2}$$

$$\frac{\partial c^-}{\partial t} = -\nabla \cdot \mathbf{J}^-,\ \mathbf{J}^- = \mathbf{u}c^- - D^-(\nabla c^- + c^- \frac{F}{RT}\nabla\phi) \tag{3}$$

$$\frac{\partial c^0}{\partial t} = -\nabla \cdot \mathbf{J}^0,\ \mathbf{J}^0 = \mathbf{u}c^0 - D^0\nabla c^0 \tag{4}$$

The diffusion coefficients of , H^+, Cl^- and water are

$D^+ = 9.312e^{-9}$ m^2 s^{-1} , $D^- = 2.032e^{-9}$ m^2 s^{-1} ,

$D^0 = 2.2e^{-9}$ m^2 s^{-1} respectively.

To these equations we must add the Stokes equation for the liquid motion,

$$\nabla \cdot \mathbf{u} = 0 \tag{5}$$

$$\rho(\frac{\partial \mathbf{u}}{\partial t} + \mathbf{u} \cdot \nabla\mathbf{u}) = \eta\nabla^2\mathbf{u} - \nabla p - q\nabla\phi \tag{6}$$

Table 1: Non dimensional parameter

Symbol	Parameter
$\tilde{x} = x/L$	Dimensionless x-coordinate
$\tilde{y} = y/L$	Dimensionless y-coordinate
$\tilde{\nabla} = L\nabla$	Dimensionless delta operator
$\tilde{\lambda}_D = \lambda_D/L$	Dimensionless Debye length
$\tilde{h} = H/L$	Height to length ratio
$\tilde{r}_e = E_1/E_2$	Electrode length ratio
$\tilde{r}_g = G_2/G_1$	Gap size ratio
$l_e = (E_1 + E_2)/L$	Equivalent length
$\tilde{t} = t/t_0, t_0 = \lambda_D L/D$	Dimensionless time
$\tilde{f} = ft_0$	Dimensionless frequency
$\tilde{c}^+ = c^+/c_{eq}$	Dimensionless concentration of cation
$\tilde{c}^- = c^-/c_{eq}$	Dimensionless concentration of anion
$\tilde{c}^0 = c^0/c_{eq}$	Dimensionless concentration of water
$\tilde{\phi} = \frac{\phi}{\phi_0}, \phi_0 = \frac{RT}{F}$	Dimensionless potential
$\tilde{A} = A/\phi_0$	Dimensionless amplitude, 0.75
$\tilde{\mathbf{u}} = \frac{\mathbf{u}}{D/L}$	Dimensionless velocity
$\tilde{p} = \frac{p}{2c^0 RT}$	Dimensionless pressure
$Ra \equiv \frac{\varepsilon}{\eta D}\left(\frac{RT}{F}\right)^2$	Rayleigh number (Ra= 0.372)
$Sc \equiv \frac{\eta}{\rho D}$	Schmidt number (Sc=348)
$\tilde{\lambda}_S = \frac{(\varepsilon/\lambda_D)}{(\varepsilon_S/\lambda_S)}$	Compact layer relative thickness

2.3 Normalization

A combination of equations 7-12 and Table 1 gives the dimensionless form of the mathematical model.

$$\tilde{\nabla}^2\tilde{\phi} = -\frac{1}{\tilde{\lambda}_D^2}\tilde{q},\qquad \tilde{q} = 0.5(\tilde{c}^+ - \tilde{c}^-) \tag{7}$$

$$\frac{\partial\tilde{c}^+}{\partial\tilde{t}} + \tilde{\lambda}_D\tilde{\nabla}\cdot\left(\tilde{\mathbf{u}}\tilde{c}^+ - \tilde{\nabla}\tilde{c}^+ + \tilde{c}^+\tilde{\nabla}\tilde{\phi}\right) = 0 \tag{8}$$

$$\frac{\partial\tilde{c}^-}{\partial\tilde{t}} + \tilde{\lambda}_D\tilde{\nabla}\cdot\left(\tilde{\mathbf{u}}\tilde{c}^- - \tilde{\nabla}\tilde{c}^- - \tilde{c}^-\tilde{\nabla}\tilde{\phi}\right) = 0 \tag{9}$$

$$\frac{\partial\tilde{c}^0}{\partial\tilde{t}} + \tilde{\lambda}_D\tilde{\nabla}\cdot\left(\tilde{\mathbf{u}}\tilde{c}^0 - \tilde{\nabla}\tilde{c}^0\right) = 0 \tag{10}$$

$$\tilde{\nabla}\cdot\tilde{\mathbf{u}}=0 \qquad (11)$$

$$\frac{1}{Sc}\left(\frac{\partial\tilde{\mathbf{u}}}{\partial\tilde{t}}+\tilde{\lambda}_D\tilde{\mathbf{u}}\cdot\tilde{\nabla}\tilde{\mathbf{u}}\right)=\tilde{\lambda}_D\tilde{\nabla}^2\tilde{\mathbf{u}}+\frac{Ra}{\tilde{\lambda}_D}\left(-\tilde{\nabla}\tilde{p}-\tilde{q}\tilde{\nabla}\tilde{\phi}\right) \qquad (12)$$

2.4 Boundary Condition

The boundary conditions at the OHP (y=0) for these functions are the continuity of the displacement vector, assuming a linear compact layer of width λ_s and permittivity ε_s

$$\frac{\varepsilon_S}{\lambda s}\Delta\phi_S=-\varepsilon\frac{\partial\phi}{\partial y} \qquad (13)$$

where $\Delta\phi_S$ denotes the voltage drop across the compact layer

$$\Delta\phi_S=V_S(x,t)-\phi(y=0) \qquad (14)$$

We assume that the electrodes are blocking to the anions,

$$D^-c^-\frac{F}{RT}\frac{\partial\phi}{\partial y}-D^-\frac{\partial c^-}{\partial y}=0 \qquad (15)$$

whereas the fluxes of positive and neutral species are related through Faradaic currents,

$$-D^+c^+\frac{F}{RT}\frac{\partial\phi}{\partial y}-D^+\frac{\partial c^+}{\partial y}=\frac{J_F}{e} \qquad (16)$$

$$-D^0\frac{\partial c^0}{\partial y}=-\frac{J_F}{e} \qquad (17)$$

To model this current we use the Butler-Volmer equation

$$\frac{J_F}{e}=K_0c^0\exp\left(\frac{\beta F\Delta\phi_S}{RT}\right)-K_+c^+\exp\left(-\frac{(1-\beta)F\Delta\phi_S}{RT}\right) \qquad (18)$$

with β as the *transfer coefficient*, where the reaction constants

$K_0 = 1e^{-10}\ m^3mol^{-1}s^{-1}$ (Reaction rate constant for water)

$K_+ = 1e^{-7}\ m^3mol^{-1}s^{-1}$ (Reaction rate constant for H^+) [13]

Note that effects due to the adsorption of movable ions is not considered.

2.5 Computational Procedure

Finite element method (FEM) is employed for solving the governing equations. Poisson, Nernst Planck, Navier-Stokes and continuity equations are solved in a time dependent domain. In this analysis, the two dimensional problem geometries are discretized by triangular mesh. Higher number of mesh elements is used on the electrode surface. This facilitates capturing the higher velocity gradient near the electrode surface arising from the no slip boundary condition.

3. RESULT AND DISCUSSION

Values of time averaged net velocity are calculated utilizing the developed non-equilibrium model. These calculated values are compared with the published numerically computed results[6]. The percentage of error for the value of calculated net velocity, $\tilde{v}$ when compared to the values of [6] for dimensionless frequency, $\tilde{f}\leq 1$ are within 0.949 %. Above $\tilde{f}=1$ the maximum error is 5.3%. So, values of dimensionless frequency is taken in the range of 0.01 to 1 in the present study. Parametric dependencies computed by present model are plotted by empty markers. The Cervenka results are represented by filled markers in Fig 2.

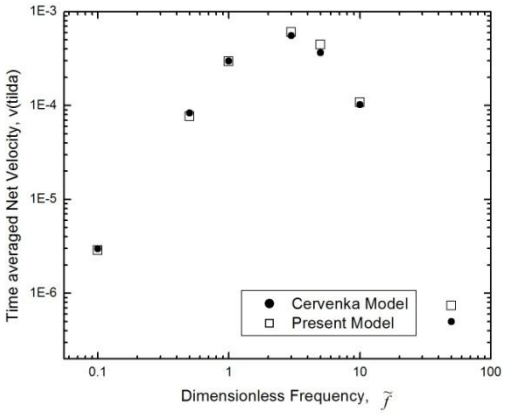

Fig 2. Comparison of present model and Cervenka model $\tilde{h}=0.333,\ \tilde{r}_e=1.667,\ \tilde{r}_g=10,\ \tilde{l}_e=0.2667,\ \tilde{A}=0.75,\ \tilde{\lambda}_D=3.3e^{-3}$

3.1 Effect of Faradaic Current

The magnitude of time averaged net velocity is shown for asymmetric arrangements of electrodes taking Faradaic currents and no Faradaic current in consideration.

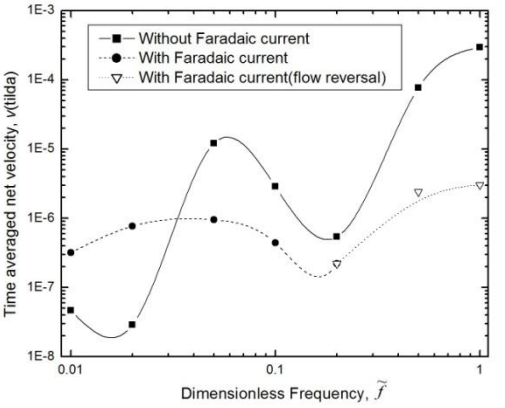

Fig 3. Effect of Faradaic current on net velocity

$\tilde{h}=0.333,\ \tilde{r}_e=1.667,\ \tilde{r}_g=10,\ \tilde{l}_e=0.2667,\ \tilde{A}=0.75,\ \tilde{\lambda}_s=4,\ \tilde{\lambda}_D=3.3e\text{-}3$

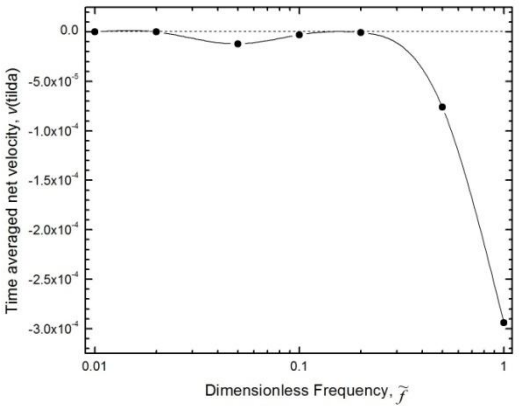

Fig 4. Net velocity without Faradaic current

$\tilde{h}=0.333,\ \tilde{r}_e=1.667,\ \tilde{r}_g=10,\ \tilde{l}_e=0.2667,\ \tilde{A}=0.75,\ \tilde{\lambda}_s=4,\ \tilde{\lambda}_D=3.3e\text{-}3$

No Faradaic currents means considering the electrodes as perfectly polarizable. Faradaic currents depolarize the electrode-electrolyte interface i.e charge leaks from the

double layer leading to lower electroosmotic velocity. This phenomenon is seen in Fig 3. Net velocity decreases by an order because of the effect of Faradaic currents. Net velocity (taken at logarithmic scale) decreases by an order because of the effect of Faradaic currents.

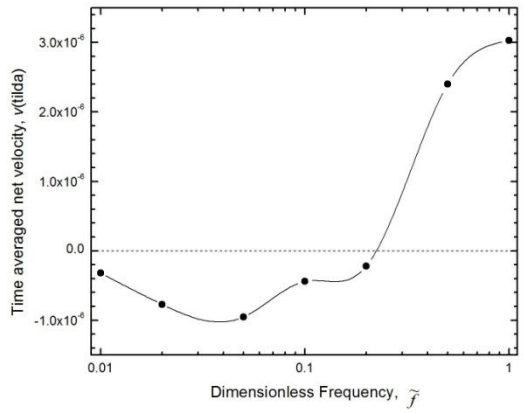

Fig 5. Net velocity with Faradaic current

$\tilde{h}$ = 0.333, $\tilde{r}_e$ = 1.667, $\tilde{r}_g$ = 10, $\tilde{l}_e$ = 0.2667, $\tilde{A}$= 0.75, $\tilde{\lambda}_s$=4 , $\tilde{\lambda}_D$=3.3e-3

No flow reversal is seen for this system when taking no Faradaic currents. Spatial direction x is taken positive from left to right side. Negative sign of velocity indicated the net flow is in the opposite direction of positive x. In the range of dimensionless frequency mentioned above in Fig 4, velocities are negative. That means fluid flows in the same direction for dimensionless frequency, ranging from 0.01 to 1while considering no Faradaic current. Flow reversal occurs at dimensionless frequency, 0.5 in this system while taking Faradaic current into consideration. Fluid velocity goes positive from negative direction as in Fig 5. In both cases, the change in the magnitude of net velocity is low upto frequency 0.2. After this frequency, net velocity significantly increases.

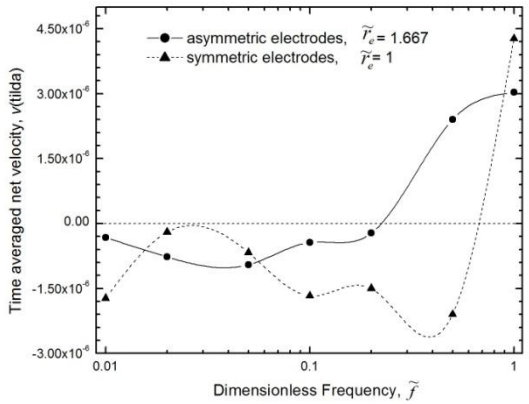

Fig 6. Comparison of net velocity for asymmetric and symmetric electrode arrangement

Net velocity comparison for asymmetric $\tilde{h}$ = 0.333, $\tilde{r}_e$ = 1.667, $\tilde{r}_g$ = 10, $\tilde{l}_e$ = 0.2667, $\tilde{A}$= 0.75, $\tilde{\lambda}_s$=4 , λ_D=3.3e^{-3} **and symmetric electrode arrangement** $\tilde{h}$ = 0.333, $\tilde{r}_e$ = 1, $\tilde{r}_g$ = 9, $\tilde{l}_e$ = 0.333 , $\tilde{A}$= 0.75, $\tilde{\lambda}_s$=4, λ_D=3.3e^{-3}

3.2 Effect of Symmetry of Electrode

Fig 6 shows the comparison of net velocity for asymmetric and symmetric electrode arrangements. In comparison of magnitude, it is seen that for lower frequency symmetric electrode arrangement exerts lower net velocity than asymmetric arrangements. For higher velocities, symmetric electrodes exert higher net velocities than asymmetric electrodes. For symmetric electrodes, flow reversal occurs at dimensionless frequency ≈ 0.6 and for asymmetric electrodes, it happens after the value of dimensionless frequency ≈ 0.2 That means flow reversal occurs at a higher frequency when electrodes are symmetric. So, symmetric electrode arrangement is a better design considering flow reversal as for a certain range of frequency, desired net flow can be obtained.

3.3 Time Average Net Velocity

Fig 7 shows time averaged net velocity in the middle plane between two electrodes. Near the electrodes the velocity increases with the increasing distance from electrode, goes to a maximum at 0.025 μm above electrodes. The maximum velocity is 0.02 μm/s for the above case of dimensionless frequency 0.3. Flow reversal is after 0.149 μm above the electrode The velocity is parabolic in shape from the point 0.0125 μm to the wall (0.33 μm).

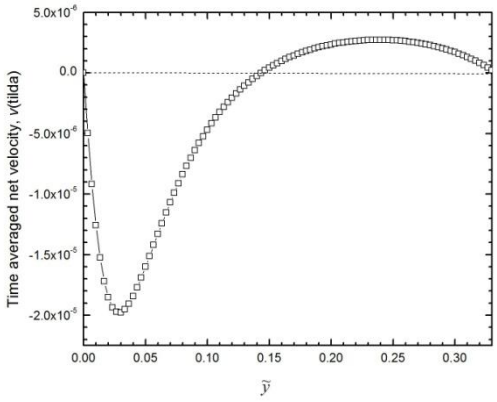

Fig 7. Time averaged net velocity vector along a vertical line at the midpoint between the electrodes

$\tilde{h}$ = 0.333, $\tilde{r}_e$ = 1, $\tilde{r}_g$ = 9 , $\tilde{l}_e$ = 0.333, $\tilde{\lambda}_D$=3.3e^{-3}, $\tilde{A}$= 0.75, $\tilde{\lambda}_s$=4, $\tilde{f}$ =0.3

3.4 Field Characteristics

Fig 8 shows the characteristics of velocity field (arrow plot), electric field (contour line) and potential field (color). Electric field is very strong between two electrodes. The velocity is maximum at the edges of the electrodes. There is a strong vortex between electrodes.

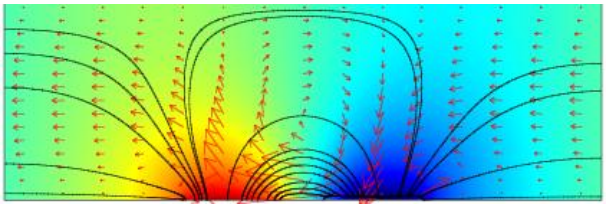

Fig 8. Net velocity comparison for asymmetric and symmetric electrode arrangement

4. CONCLUSION

A fully nonlinear analysis is performed here to understand the mechanism of ac electroosmosis with Faradaic currents. Net velocity without Faradaic current

surpasses net velocity with Faradaic current and remains higher throughout the entire domain. Changes in velocity profile are sharper for Faradaic current than no Faradaic current. In the same region of frequency, flow reversal occurs while taking Faradaic current into consideration where no flow reversal occurs without Faradaic current. Taking absolute value of net velocity, symmetric electrode arrangement exerts lower net velocity than asymmetric arrangements at lower frequency. For higher velocities, symmetric electrodes exert higher net velocities than asymmetric electrodes. For symmetric electrodes, flow reversal occurs at dimensionless frequency = 0.6 and for asymmetric electrodes, it happens after the value of dimensionless frequency =0.2.

5. REFERENCES

1. Green, N.G., Ramos, A., Morgan, H., and Castellanos A., 2000, "Fluid flow induced by nonuniform ac electric fields in electrolytes on microelectrodes. I. Experimental measurements," The American Physical Society, 61:4
2. Gonzalez, A., Ramos, A., Green, N. G., Castellanos, A. and Morgan, H., 2000, "Fluid flow induced by nonuniform ac electric fields in electrolytes on microelectrodes.II. A linear double-layer analysis," The American Physical Society, 61:4
3. Green, N.G., Ramos, A., Gonzalez, A., Morgan, H. and Cstellanos, A., 2002, "Fluid flow induced by nonuniform ac electric fields in electrolytes on microelectrodes. I. Observations of streamlines and numerical simulation," The American Physical Society, Physical Review E, 66(4):026305
4. Squires, T. M. and Bazant, M. Z., 2004, "Induced charge electro-osmosis," Journal of Fluid Mechanics, 509:217-252
5. Hrdlicka, J., Cervenka, P., Pribyl, M. and Snita, D., 2010, "Mathematical modeling of AC electroosmosis in microfluidic and nanofluidic chips using equilibrium and non-equilibrium approaches," Journal of Appl Electrochem, 40:967-980
6. Hrdlicka, J., Cervenka, P., Pribyl, M. and Snita, D., 2010, "Toward high net velocities in AC electroosmosis micropumps based on asymmetric coplanar electroes", IEEE transactions on industry applications, 46:5
7. Gonzalez, A., Ramos, A., Sanchez, P. G. and Castellanos, A., 2010, "Effect of the combinded action of Faradaic currents and mobility differences in ac electroosmosis", The American Physical society, Physical Review E, 81:016320
8. Bazant, M. Z., Squires, T. M., 2004, "Induced-Charge electrokinetic phenomena: theory and microfluidin applications," The American Physical society, 92(6)
9. Pribyl, M. and Adamiak, K., 2010, "Numerical Models for AC Electroosmotic Micropumps," IEEE Transactions on Industry Applications, 46(6)
10. Cervenka, P., Hrdlicka, J., Pribyl, M. and Snita, D., 2010, "Study on Faradaic and Coulombic interactions at microelectrodes utilized in AC electroosmotic micropumps", Research work of Institute of Chemical Technology, Prague, Department of Chemical Engineering, Technick´a 5, 166 28 Praha 6, Czech Republic, MSMT no. 21.
11. Ramos, A., González, A., García-Sánchez, P. and Castellanos, A., 2007, "A linear analysis of the effect of Faradaic currents on traveling-wave electroosmosis", Journal of Colloid and Interface Science, 309:323–331
12. García-Sánchez, P., Ramos, A., González, A., 2011, "Effects of Faradaic currents on AC electroosmotic flows with coplanar symmetric electrodes",Colloids and Surfaces A:Physicochem. Eng. Aspects, 376: 47–52
13. González, A., Ramos, A., García-Sánchez, P. and 2 and Castellanos, A., 2010," Effect of the combined action of Faradaic currents and mobility differences in ac electro-osmosis", Physical Review E, 81: 016320.

6. NOMENCLATURE

Symbol	Meaning	Unit
A	Amplitude	(A)
c	Concentration	(mol m^{-3})
D	Diffusivity	(m^2s^{-1})
f	Frequency	(s^{-1})
F	The Faraday constant	($Cmol^{-1}$)
H	Micro channel height	(m)
L	Length of periodic segment	(m)
G	Gap size	(m)
E	Electrode size	(m)
n	Normal unit vector	
p	Pressure	Pa
R	Molar gas constant	($JK^{-1}mol^{-1}$)
t	Time	(s)
T	Temperature	(K)
u	Net velocity	(ms^{-1})
$\hat{\mathbf{u}}$	Time averaged net velocity	(ms^{-1})
x	Spatial coordinate	(m)
y	Spatial coordinate	(m)
ε	Electrolyte permittivity	(Fm^{-1})
ϕ	Electric potential	(V)
η	Dynamic viscosity	(PaS)
λ_D	The Debye length	(m)
λ_s	Compact layer width	(m)
q	Space charge density	Cm^{-3}
β	Transfer coefficient	
J	Flux	Cm^{-2}

8. MAILING ADDRESS:

Noor Quddus
Department of Mechanical Engineering
Bangladesh University of Engineering and Technology, Dhaka-1000, Bangladesh
E-mail: nquddus@me.buet.ac.bd

Proceedings of the
International Conference on Mechanical Engineering 2011
(ICME2011) 18-20 December 2011, Dhaka, Bangladesh

ICME 11–225